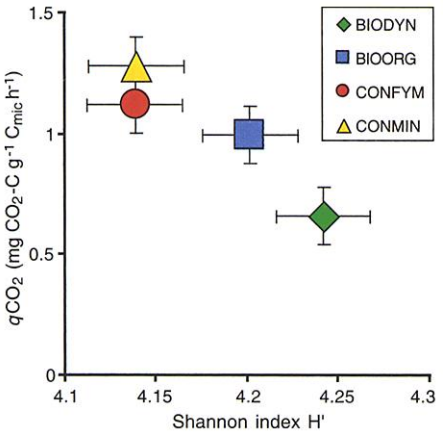

Fig. 4. Soil microbial functional diversity (Shannon index H') and metabolic quotient (qCO_2 = soil basal respiration/soil microbial biomass) correlate inversely. A higher diversity in the organic plots is related to a lower qCO_2, indicating greater energy efficiency of the more diverse microbial community. The Shannon index is significantly different between both conventional systems (CONFYM, CONMIN) and the BIODYN system, the qCO_2, between CONMIN and BIODYN ($P < 0.05$).

with an increased diversity in organic soils transform carbon from organic debris into biomass at lower energy costs, building up a higher microbial biomass. Accordingly, the functional role of diverse plant communities in soil nitrate utilization has been quoted (*24*), as well as the significance of mycorrhizal diversity for phosphorus uptake and plant productivity (*25*). The consistent results of these two studies (*24*, *25*) and our own within the soil-plant system support the hypothesis that a more diverse community is more efficient in resource utilization. The improvement of biological activity and biodiversity below and above ground in initial stages of food webs in the DOK trial is likely to provide a positive contribution toward the development of higher food web levels including birds and larger animals.

The organic systems show efficient resource utilization and enhanced floral and faunal diversity, features typical of mature systems. There is a significant correlation ($r = 0.52$, $P < 0.05$) between above-ground (unit energy per unit crop yield) and below-ground (CO_2 evolution per unit soil microbial biomass) system efficiency in the DOK trial. We conclude that organically manured, legume-based crop rotations utilizing organic fertilizers from the farm itself are a realistic alternative to conventional farming systems.

References and Notes

1. D. Pimentel *et al.*, *Science* **267**, 1117 (1995).
2. D. Tilman, *Proc. Nat. Acad. Sci. U.S.A.* **96**, 5995 (1999).
3. D. Pimentel *et al.*, *Bioscience* **47**, 747 (1997).
4. www.organic.aber.ac.uk/stats.shtml
5. L. E. Drinkwater, P. Wagoner, M. Sarrantonio, *Nature* **396**, 262 (1998).
6. J. P. Reganold, J. D. Glover, P. K. Andrews, H. R. Hinman, *Nature* **410**, 926 (2001).
7. P. Mäder, S. Edenhofer, T. Boller, A. Wiemken, U. Niggli, *Biol. Fertil. Soils* **31**, 150 (2000).
8. P. Simon, Landwirtschaftliches Zentrum Ebenrain, CH-4450 Sissach/BL, personal communication.
9. F. Offermann, H. Nieberg, *Economic Performance of Organic Farms in Europe* (University of Hohenheim, Hago Druck & Medien, Karlsbad-Ittersbach, Germany, 2000), vol. 5.
10. T. Alföldi *et al.*, unpublished observations.
11. S. Siegrist, D. Schaub, L. Pfiffner, P. Mäder, *Agric. Ecosys. Environ.* **69**, 253 (1998).
12. F. Schinner, R. Öhlinger, E. Kandeler, R. Margesin, *Bodenbiologische Arbeitsmethoden* (Springer Verlag, Berlin Heidelberg, ed. 2, 1993).
13. A. Oberson, J.-C. Fardeau, J.-M. Besson, H. Sticher, *Biol. Fertil. Soils* **16**, 111 (1993).
14. A. Oberson, J.-M. Besson, N. Maire, H. Sticher, *Biol. Fertil. Soils* **21**, 138 (1996).
15. F. Oehl *et al.*, *Biol. Fertil. Soils* **34**, 31 (2001).
16. S. E. Smith, D. J. Read, *Mycorrhizal Symbiosis* (Academic Press, London, ed. 2, 1997).
17. L. Pfiffner, P. Mäder, *Biol. Agric. Hortic.* **15**, 3 (1997).
18. L. Pfiffner, U. Niggli, *Biol. Agric. Hortic.* **12**, 353 (1996).
19. A. Flieβbach, P. Mäder, in *Microbial Communities—Functional versus Structural Approaches*, H. Insam, A. Rangger, Eds. (Springer, Berlin, 1997), pp. 109–120.
20. E. P. Odum, *Science* **164**, 262 (1969).
21. H. Insam, K. Haselwandter, *Oecologia* **79**, 174 (1989).
22. A. Flieβbach, P. Mäder, U. Niggli, *Soil Biol. Biochem.* **32**, 1131 (2000).
23. A. Flieβbach, P. Mäder, *Soil Biol. Biochem.* **32**, 757 (2000).
24. D. Tilman, D. Wedin, J. Knops, *Nature* **379**, 718 (1996).
25. M. G. A. van der Heijden *et al.*, *Nature* **396**, 69 (1998).
26. We sincerely thank all co-workers in the DOK trial, especially W. Stauffer and R. Frei and the farmer groups. We also thank T. Boller and A. Wiemken and two unknown referees for their helpful comments. This work was supported by the Swiss Federal Office for Agriculture and the Swiss National Science Foundation.

Supporting Online Material

www.sciencemag.org/cgi/content/full/296/5573/1694/DC1
Materials and Methods
Fig. S1
Tables S1 to S5

21 February 2002; accepted 26 April 2002

Control of Stomatal Distribution on the *Arabidopsis* Leaf Surface

Jeanette A. Nadeau and Fred D. Sack*

Stomata regulate gas exchange and are distributed across the leaf epidermis with characteristic spacing. *Arabidopsis* stomata are produced by asymmetric cell divisions. Mutations in the gene *TOO MANY MOUTHS* (*TMM*) disrupt patterning by randomizing the plane of formative asymmetric divisions and by permitting ectopic divisions. *TMM* encodes a leucine-rich repeat–containing receptor-like protein expressed in proliferative postprotodermal cells. TMM appears to function in a position-dependent signaling pathway that controls the plane of patterning divisions as well as the balance between stem cell renewal and differentiation in stomatal and epidermal development.

Stomata allow gas exchange and thus are key to the survival of land plants, yet the genes controlling stomatal development are poorly understood (*1*, *2*). Both the number and distribution of stomata are regulated during leaf development. Stomata are formed after a series of asymmetric divisions of transiently self-renewing precursors termed meristemoids [fig. S1 (*3*)]. Stomata are continually produced during the mosaic development of the leaf, and many form by division of cells next to preexisting stomata (Fig. 1A). Correct spacing results when the plane of formative asymmetric divisions is oriented so that the new precursor, the satellite meristemoid, does not contact the preexisting stoma or precursor (*1*, *4*). Intercellular signaling provides spatial cues that regulate division orientation and may also block asymmetric division in cells adjacent to two stomata or precursors (*4*). The recessive *too many mouths* (*tmm*) mutation randomizes the plane of asymmetric division in cells next to a single stoma or precursor and permits asymmetric divisions in cells next to two stomata or precursors, thus producing clusters of stomata (Fig. 1, A and C). Also, *tmm* meristemoids divide fewer times before assuming the determinate guard mother cell fate. These phenotypes suggest that TMM is required for cells to respond appropriately to their position during stomatal development and that TMM participates in intercellular signaling.

With the use of positional cloning (*3*), *TMM* was found to encode a leucine-rich repeat (LRR)–containing receptor-like protein of 496 amino acids with a molecular weight of ~54 kD (Fig. 2A). The predicted protein product contains 10 uninterrupted plant-type LRRs (*5*) and a putative COOH-terminal transmembrane domain. *TMM* en-

Department of Plant Biology, Ohio State University, 1735 Neil Avenue, Columbus, OH 43210, USA.

*To whom correspondence should be addressed. E-mail: sack.1@osu.edu

codes a predicted signal peptide of 23 amino acids and is most likely targeted to the plasma membrane (*6*). The LRR motif is found in proteins with a variety of functions in prokaryotes and eukaryotes, where it facilitates protein-protein or protein-ligand interactions. In transmembrane receptors, the LRR motif typically recognizes an extracellular signal and transduces information across the membrane through activation of a cytoplasmic kinase domain. Plant LRR receptor-like kinases (LRR-RLKs) participate in signaling during plant development, including meristem maintenance by CLAVATA1 (CLV1), hormone perception by BRASSINOSTEROID INSENSITIVE1 (BRI1), regulation of organ shape, and abscission zone formation (*7*–*10*); they also function in disease resistance (*11*, *12*).

TMM lacks a cytoplasmic kinase domain and thus is similar to LRR-containing receptor-like proteins (LRR-RLPs), including CLV2 (*13*). Overall homology to previously described LRR-RLPs is relatively low, with the most homology between TMM and tomato disease resistance proteins, encoded by *Cf-2* and *Cf-9* (*14*, *15*), even though TMM has no known role in disease resistance. TMM contains paired cysteines in the NH_2- and COOH-terminal non-LRR regions (four and two cysteines, respectively) that may form intra- or intermolecular disulfide linkages with a partner such as an LRR-RLK, similar to the association of CLV1 with CLV2 in a receptor complex (*16*). Presumably, interaction with additional factors would be necessary for TMM to participate in a signaling cascade, because it lacks a cytoplasmic domain.

The ethyl methane sulfonate–induced *tmm-1* mutation (*17*) involves an insertion of a single thymidine in position 986 of the *TMM* coding region, and the fast-neutron mutagenized *tmm-2* mutation has a deletion of a single thymidine at position 992. These mutations result in 33 and 14 missense residues, respectively, before premature termination that removes two-and-a-half LRR repeats and the transmembrane domain. Although it is likely that these mutant proteins do not function, shortened versions of TMM could be secreted from cells and may retain some activity. This possibility is supported by partial activity of the truncated protein product encoded by the rice disease resistance gene *Xa21D*, which lacks the normal transmembrane and kinase domains (*18*).

Monocot and other dicot species each encode TMM-like gene products. These proteins are most similar to TMM in the NH_2-terminal, non-LRR–encoding domain (NNL) (Fig. 2B). In this region, the tomato protein is 75% and the rice protein is 60% identical to TMM, whereas they are 65 and 51% identical, respectively, to TMM within the LRR region. In contrast, the *Arabidopsis* genome encodes a small family of TMM-like RLPs, but these proteins are no more than 32% identical overall, and the NNL domain is not well conserved. Strong conservation of TMM-like proteins, especially the NNL, suggests that a biochemical function arose before the divergence of monocots and dicots, although grasses lack satellite meristemoids. Because *tmm* eliminates stomata in several *Arabidopsis* organs (*19*), TMM may participate in the initiation of asymmetric divisions that form stomata in all plants.

TMM transcripts are present in developing shoots but not in roots (Fig. 2C). The absence of transcripts from roots and the normal phenotype of *tmm* roots suggest that *TMM* does not participate in patterning asymmetric divisions of the root. As shown by hybridization to RNA isolated from rosette leaves of Columbia wild-type, *tmm-1*, and *tmm-2* plants, *TMM* is transcribed at roughly equivalent levels in wild-type and mutant plants.

The cellular pattern of expression was determined by means of TMM translational fusions with green fluorescent protein (GFP) driven by the native *TMM* promoter (Fig. 3). Both COOH- and NH_2-terminal TMM fusion proteins mostly or completely complemented the *tmm* phenotype, indicating that both the pattern of expression and protein activity are sufficient to restore developmental function (table S1). Expression was found in shoot epidermal cells and not in the shoot apical meristem, in subepidermal layers of the shoot, or in roots. In developing leaves, expression was first detected in young leaf primordia (Fig. 3A), and then migrated basipetally during development. The number of GFP-TMM–positive cells declined as leaves matured, and none were observed in fully expanded leaves. The absence of shoot apical meristem defects in *tmm* mutant plants, coupled with the lack of *TMM* expression in L1 cells of the meristem or incipient leaf primordia, indicates that TMM is not involved in protodermal cell development but instead de-

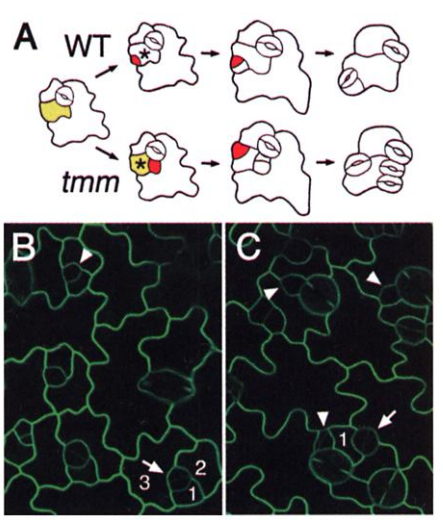

Fig. 1. Stomatal pattern development. (**A**) An idealized wild-type (WT) series (top) compared to an actual series from a *tmm* mutant plant (bottom). Methods are given in (*4*). Asymmetric division of a meristemoid mother cell (yellow) produces a meristemoid (red). An oriented division in a neighbor cell places the satellite meristemoid away from the preexisting stoma. *tmm* disrupts this division orientation, permits cells next to two stomata/precursors (*) to divide asymmetrically, and reduces the number of meristemoid divisions. (**B** and **C**) Cell membrane–localized GFP (PIP2A) in developing wild-type (B) and *tmm-1* (C) leaves. Meristemoids (arrowheads) are normally placed in the wild type and can be ectopically placed in *tmm* mutants. The young stoma [arrow in (B)] probably formed after three asymmetric divisions that also produced the three surrounding epidermal cells (the cell labeled 1 is most recent). The *tmm* stoma [arrow in (C)] was produced after a single asymmetric division. Division of a cell next to two stomata/precursors produced an ectopic satellite meristemoid (arrowhead left of cell 1).

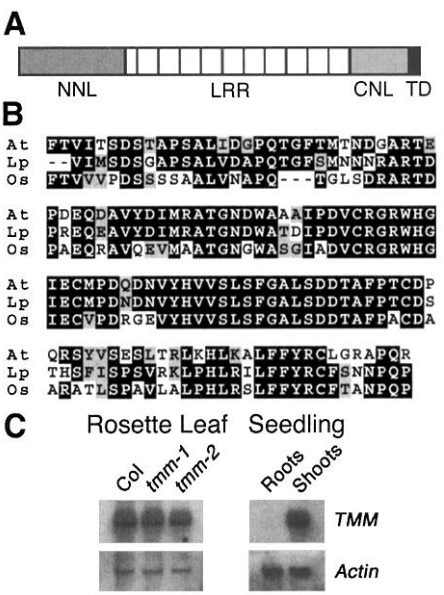

Fig. 2. Molecular analysis of *TMM*. (**A**) The mature protein includes 10 LRRs, an NNL, a COOH-terminal non-LRR domain (CNL), a predicted transmembrane domain (TD), and no apparent cytoplasmic residues. (**B**) Alignment of the NNL domain of *Arabidopsis* TMM (At) with putative orthologs from *Lycopersicon pennelli* (Lp) and *Oryza sativa* cv. Nipponbare (Os). GenBank accession numbers are NC003070, AW160186, and AP002819, respectively. Gray shading indicates conserved residues; black shading shows identical residues (*22*). (**C**) Northern analysis of *TMM* expression in developing rosette leaves of 3-week-old Columbia (Col) wild-type, *tmm-1*, and *tmm-2* plants, and roots and shoots from 9-day-old agar-grown wild-type seedlings, shows a transcript of ~1.6 kb. *TMM* signal was not detected in roots. Actin serves as a loading control.

fines a postprotodermal phase of epidermal development.

Because *tmm* disrupts the plane and frequency of asymmetric divisions in neighbor cells (cells next to stomata, meristemoids, or guard mother cells), TMM expression was analyzed in these locations. TMM is expressed in many neighbor cells (Fig. 3, C through I). This localization is consistent with phenotypic data (*4*), suggesting that TMM functions in an intercellular signaling pathway in which neighbor cells receive cues about the position of an adjacent stoma or precursor. A putative receptor complex containing TMM could transduce extracellular spatial information into a signaling cascade that orients the plane of asymmetric division, thus generating the minimal one-celled stomatal spacing pattern.

Although TMM is expressed in neighbor cells, not all such cells were fluorescent (Fig. 3, C through I). To determine whether this reflects a developmental pattern, TMM expression was quantified as a function of neighbor cell age (Fig. 4). Expression was highest in the neighbor cell most recently produced by asymmetric division and declined progressively with age. Because young neighbor cells are more likely to divide asymmetrically than older ones (*1*, *2*), TMM expression correlates positively with division competence and negatively with the terminal differentiation of neighbor cells as pavement cells. TMM is also expressed in some cells adjacent to two stomata and/or precursors (asterisks in Fig. 3G), suggesting that TMM may help prohibit their division. TMM expression does not, however, predict the formative asymmetric division of neighbor cells. About 40% of complexes do not produce any satellite meristemoids, and only 12% of all complexes produce more than one satellite meristemoid (*20*), but most complexes exhibit TMM-GFP fluorescence in more than one neighbor cell (Fig. 4). This indicates that TMM is not restricted to cells committed to asymmetric division but is expressed in some cells that remain nonproliferative or divide symmetrically.

Smaller cells in developing leaves can divide either symmetrically or asymmetrically, and only the latter produces a meristemoid (*4*). TMM was often expressed in relatively small cells that were not neighbor cells (arrow in Fig. 3D; arrowheads in Fig. 3H). These cells did not appear to be meristemoids because of their shape and because there was no adjacent larger sister cell. TMM expression may thus mark a population of division-competent stem cells from which the stomatal lineage may be selected. This hypothesis is supported by the observation that larger epidermal cells, which are known to divide rarely if at all (*4*, *21*), usually did not express TMM (Fig. 3, C through I).

TMM is also expressed in stomatal precursor cells. Expression is highest in meristemoids, less abundant in guard mother cells, and absent from mature guard cells (Fig. 3, D through I). Meristemoids have only a limited capacity for self-renewal and ultimately differentiate into guard mother cells. TMM regulates meristemoid self-renewal, because *tmm* reduces the number of meristemoid asymmetric divisions (*4*). In addition, meristemoids that occasionally form in contact divide away from each other in the wild type but not in *tmm* mutants (*4*). These phenotypes and the strong expression of TMM in meristemoids suggest that TMM regulates proliferation and positional responses in meristemoids as well as in division-competent cells that may enter the stomatal pathway.

On the basis of these observations and the identity of TMM as an LRR-RLP, we propose that TMM is a component of a receptor complex whose function is to sense positional cues during epidermal development. The interspersion of proliferating and differentiating cells during this phase requires that spatial information be integrated to appropriately

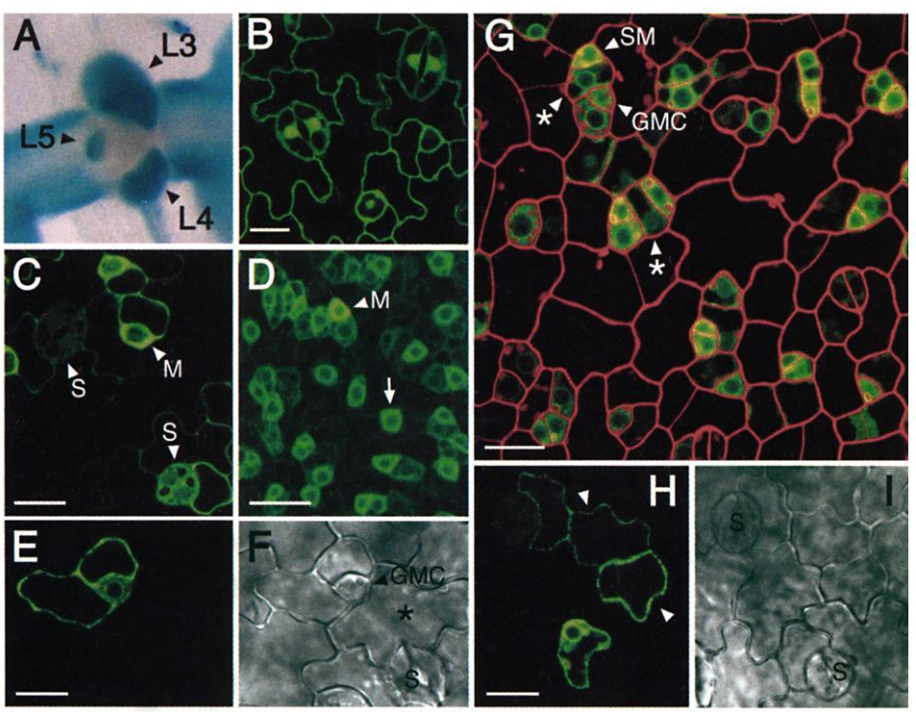

Fig. 3. *TMM* expression pattern in wild-type plants. All fluorescence images are confocal micrographs of the developing abaxial leaf epidermis. (**A**) The *TMM* promoter drives expression in developing leaves (L3 through L5) but not in the shoot apical meristem or incipient primordia. GUS staining is from *TMMpro::GUS-GFP*. (**B**) Control (*CaMV 35S::GFP*) showing constitutive cytoplasmic and nuclear fluorescence. Fluorescence appears localized to the cell periphery because of the large vacuole present in epidermal cells. (**C**) Cell-specific expression including that in a stoma (S) and meristemoid (M) from *TMMpro::GUS-GFP* [see supporting online text (*3*)]. (D through I) *TMMpro::TMM-GFP* fusion protein. (**D**) Young leaf undergoing the initial asymmetric divisions that form meristemoids (M), which are brighter. Meristemoids, as well as isolated cells (arrow), may later host an asymmetric division. Fluorescence appears diffuse in very young cells because of the distribution of endoplasmic reticulum. Paired fluorescence (**E**) and bright-field (**F**) images of a guard mother cell (GMC) complex with two TMM-GFP–positive neighbor cells and one negative neighbor cell (*). Stomatal (S) fluorescence is absent. (**G**) Intermediate stage leaf showing dispersed TMM-GFP–positive cells, many produced by asymmetric divisions. A satellite meristemoid (SM) was formed by division of the neighbor cell adjacent to a guard mother cell (GMC). Cells next to more than one stoma or precursor rarely divide (*). Cell walls were visualized with propidium iodide. Paired fluorescence (**H**) and bright-field (**I**) micrographs showing stomatal complexes in which only the most recently formed sister cell to a stoma (S) is TMM-GFP–positive. Two cells that are not adjacent to stomata or precursors are also fluorescent [arrowheads in (H)]. Scale bars, 14 μm.

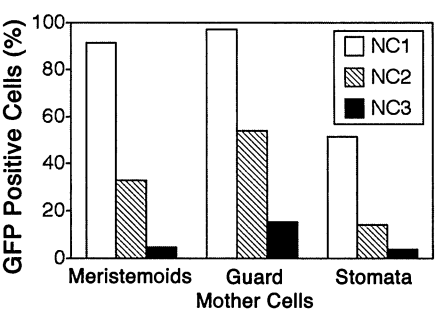

Fig. 4. TMM-GFP expression as a function of neighbor cell size and location next to meristemoids, guard mother cells, or stomata. Expression was most frequent in the smallest neighbor cell (NC1) at all stages and decreased in all NCs with age. Data were collected from the abaxial epidermis of intermediate-stage second leaves.

pattern cell types. TMM controls the orientation of asymmetric divisions that create the minimal one-celled stomatal spacing pattern and may also participate broadly in regulating cell proliferation and differentiation based on positional context. The latter function appears analogous to the CLV1/CLV2 signaling pathway that regulates the balance between stem cell maintenance in the central shoot apical meristem and cell differentiation at the meristem flanks (*9*). In contrast, TMM functions in cells that are dispersed within the developing epidermis and have different fate potentials, ranging from multipotent stem cells that may undergo a formative asymmetric division to meristemoids that invariably mature into stomata.

Additional support for the importance of position-dependent cell proliferation in epidermal patterning comes from the *STOMATAL DENSITY AND DISTRIBUTION 1* locus, which encodes a processing protease likely to participate in cell signaling (*1*). The control of cell division relative to nearby differentiating cells is likely to be a recurring theme in plant development.

References and Notes

1. D. Berger, T. Altmann, *Genes Dev.* **14**, 1119 (2000).
2. J. A. Nadeau, F. D. Sack, in *The* Arabidopsis *Book*, C. R. Somerville, E. M. Meyerowitz, Eds. (American Society of Plant Biologists, Rockville, MD, 2002), www.aspb.org/publications/arabidopsis
3. Supplemental materials and methods are available on *Science* Online at www.sciencemag.org/cgi/content/full/296/5573/1697/DC1.
4. M. D. Geisler, J. A. Nadeau, F. D. Sack, *Plant Cell* **12**, 2075 (2000).
5. A. V. Kajava, *J. Mol. Biol.* **277**, 519 (1998).
6. K. Nakai, M. Kanehisa, *Genomics* **14**, 897 (1992).
7. T.-L. Jinn, J. M. Stone, J. C. Walker, *Genes Dev.* **14**, 108 (2000).
8. K. U. Torii *et al.*, *Plant Cell* **8**, 735 (1996).
9. S. E. Clark, R. W. Williams, E. M. Meyerowitz, *Cell* **89**, 575 (1997).
10. J. Li, J. Chory, *Cell* **90**, 929 (1997).
11. L. Gomez-Gomez, T. Boller, *Mol. Cell* **5**, 1003 (2000).
12. G.-L. Wang, W.-H. Song, D.-L. Ruan, S. Sideris, P. C. Ronald, *Mol. Plant Microbe Interact.* **9**, 850 (1996).
13. S. Jeong, A. E. Trotochaud, S. E. Clark, *Plant Cell* **11**, 1925 (1999).
14. D. A. Jones, C. M. Thomas, K. E. Hammond-Kosack, P. J. Balint-Kurti, J. D. G. Jones, *Science* **266**, 789 (1994).
15. M. S. Dixon *et al.*, *Cell* **84**, 451 (1996).
16. A. E. Trotochaud, T. Hao, G. Wu, Z. Yang, S. E. Clark, *Plant Cell* **11**, 393 (1999).
17. M. Yang, F. D. Sack, *Plant Cell* **7**, 2227 (1995).
18. G.-L. Wang *et al.*, *Plant Cell* **10**, 765 (1998).
19. M. Geisler, M. Yang, F. D. Sack, *Planta* **205**, 522 (1998).
20. M. J. Geisler, J. A. Nadeau, F. D. Sack, unpublished data.
21. P. M. Donnelly, D. Bonetta, H. Tsukaya, R. E. Dengler, N. G. Dengler, *Dev. Biol.* **215**, 407 (1999).
22. Single-letter abbreviations for the amino acid residues are as follows: A, Ala; C, Cys; D, Asp; E, Glu; F, Phe; G, Gly; H, His; I, Ile; K, Lys; L, Leu; M, Met; N, Asn; P, Pro; Q, Gln; R, Arg; S, Ser; T, Thr; V, Val; W, Trp; and Y, Tyr.

23. We are grateful to M. Bolgar and C. Lee for technical assistance, to M. Geisler for Fig. 1A, and to B. Ding for the use of his confocal microscope. S. Cutler, D. Ehrhardt, and C. Somerville generously provided the GFP-PIP2A line. Funded by NSF grant IBN-9904826 to F.D.S and J.A.N.

7 January 2002; accepted 23 April 2002

Probing Protein Electrostatics with a Synthetic Fluorescent Amino Acid

Bruce E. Cohen,[1]† Tim B. McAnaney,[2]* Eun Sun Park,[2]* Yuh Nung Jan,[1] Steven G. Boxer,[2] Lily Yeh Jan[1]

Electrostatics affect virtually all aspects of protein structure and activity and are particularly important in proteins whose primary function is to stabilize charge. Here we introduce a fluorescent amino acid, Aladan, which can probe the electrostatic character of a protein at multiple sites. Aladan is exceptionally sensitive to the polarity of its surroundings and can be incorporated site-selectively at buried and exposed sites, in both soluble and membrane proteins. Steady-state and time-resolved fluorescence measurements of Aladan residues at different buried and exposed sites in the B1 domain of protein G suggest that its interior is polar and heterogeneous.

High-resolution structures provide the primary basis for analysis of protein function, yet investigations into other physical properties such as protein dynamics and electrostatics have been hampered by experimental limitations. For electrostatics in particular, the lack of general techniques for measuring static and dynamic electric fields within a protein has made it difficult to address even a most basic question: how polar is a protein? A protein's polarity—that is, its capacity to solvate charge—affects the strengths of all electrostatic interactions within the protein, as well as the strengths of interactions with proteins, substrates, and other ligands, making it a critical determinant of protein structure, stability, and, ultimately, activity (*1*, *2*). Ideas about the polarity of the protein interior have progressed from simple models of proteins as nonpolar and homogeneous, described by a low dielectric constant (i.e., $\varepsilon = 2$ to 4), to more complex models that consider sources of local heterogeneity. Computational models suggest that local dielectric properties can vary considerably and, in some cases, correspond to polar solvents, even in the protein interior (*1*, *3*). Examining protein solvation experimentally has usually relied on the fortuitous affinity of probes for ligand-binding sites (*4*–*9*) or the presence of endogenous long-wavelength chromophores (*10*, *11*), typically limiting such measurements to individual, sometimes ill-defined, locations within particular proteins. Tryptophan fluorescence has also been used as an intrinsic local environmental probe (*12*, *13*), but tryptophan's utility is limited by its complex photophysics. An ideal probe for studying protein dynamics and electrostatics would be sensitive to its environment and could be incorporated site-specifically throughout any protein of interest. Toward that end, we have synthesized an environment-sensitive fluorescent amino acid, Aladan, and incorporated it site-specifically into proteins by both nonsense suppression and solid-phase synthesis, and we have used it to probe the electrostatic character of the B1 domain of streptococcal protein G (GB1) at multiple sites by steady-state and time-resolved fluorescence.

The fluorophore 6-dimethylamino-2-acylnaphthalene (DAN) undergoes a large charge redistribution upon excitation and has nearly ideal environment sensor properties (*4*, *5*, *12*, *14*). As shown in Fig. 1, an alanine derivative of DAN (Aladan, compound 3) (*15*) was synthesized and either converted to its Fmoc derivative (compound 4) for solid-phase peptide synthesis or functionalized (compound 5) for coupling to a *T. thermophila* suppressor tRNA (*16*) for nonsense suppression. The bisamide *N*-acetyl-Aladanamide (NAAA, Fig. 1B, inset) mimics Aladan within a peptide and exhibits a similar solvatochromism as observed for other DAN probes (*12*, *14*), including a large shift in emission maximum (λ_{max}) that depends on solvent polarity (from 409 nm in heptane to 542 nm in water), as well as emission at longer wavelengths in hydroxylated solvents relative to those of aprotic solvents of comparable polarities (Fig. 1, B and C). Other spectral characteristics such as absorption show much less dramatic changes (*17*). The λ_{max} of NAAA in water is not sensitive to changes in pH be-

[1]Howard Hughes Medical Institute and Departments of Physiology and Biochemistry, University of California San Francisco, San Francisco, CA 94143, USA. [2]Department of Chemistry, Stanford University, Stanford, CA 94305, USA.

*These authors contributed equally to this work.
†To whom correspondence should be addressed. Email: bcohen@itsa.ucsf.edu